J|A|C|S ARTICLES

Published on Web 10/13/2009

Proton Transfer in Guanine−Cytosine Radical Anion Embedded in B-Form DNA

Hsing-Yin Chen,* Chai-Lin Kao, and Sodio C. N. Hsu

Department of Medicinal and Applied Chemistry and Center of Excellence for Environmental Medicine, Kaohsiung Medical University, Kaohsiung 807, Taiwan

Received August 20, 2009; E-mail: hychen@kmu.edu.tw

Abstract: The electron-attachment-induced proton transfer in the guanine−cytosine (G:C) base pair is thought to be relevant to the issues of charge transport and radiation damage in DNA. However, our understanding on the reaction mainly comes from the data of isolated bases and base pairs, and the behavior of the reaction in the DNA duplex is not clear. In the present study, the proton-transfer reaction in reduced G:C stacks is investigated by quantum mechanical calculations with the aim to clarify how each environmental factor affects the proton transfer in G:C$^{\bullet-}$. The calculations show that while the proton transfer in isolated G:C$^{\bullet-}$ is exothermic with a small energetic barrier, it becomes endothermic with a considerably enhanced energetic barrier in G:C stacks. The substantial effect of G:C stacking is proved to originate from the electrostatic interactions between the dipole moments of outer G:C base pairs and the middle G:C$^{\bullet-}$ base-pair radical anion; the extent of charge delocalization is very small and plays little role in affecting the proton transfer in G:C$^{\bullet-}$. On the basis of the electrostatic model, the sequence dependence of the proton transfer in the ionized G:C base pair is predicted. In addition, the water molecules in the first hydration shell around G:C$^{\bullet-}$ display a pronounced effect that facilitates the proton-transfer reaction; further consideration of bulk hydration only slightly lowers the energetic barrier and reaction energy. We also notice that the water arrangement around an embedded G:C$^{\bullet-}$ is different from that around an isolated G:C$^{\bullet-}$, which could result in a very different solvent effect on the energetics of the proton transfer. In contrast to the important influences of base stacking and hydration, the effects of sugar−phosphate backbone and counterions are found to be minor. Our calculations also reveal that a G:C base pair embedded in DNA is capable of accommodating two excess electrons only in bulk hydration; the resultant G(N1−H)$^-$:C(N3+H)$^-$ dianion is stable and exists long enough to lead to DNA damage. The combination of the present results with the previous findings in literature suggests that the behaviors of charge transport and low-energy electron-induced damage in DNA are highly susceptible to the hydration level.

1. Introduction

Proton transfer in DNA base pairs plays important roles in many biological and chemical phenomena and processes, such as genetic mutation,[1,2] radiation-induced DNA damage,[3,4] specific photostability of Watson−Crick structure,[5−8] and dynamics of charge transfer in DNA,[9−11] and, therefore, has become a subject of continuous interest for both experimental and theoretical research. In general, while the proton transfer for DNA base pairs in neutral electronic ground state is energetically unfavorable,[12−15] explaining why the genetic code is so stable, external stimuli that lead to the modifications of electronic states might promote the proton-transfer reaction in base pairs.[16−22]

When DNA is subjected to high-energy radiation, positive holes and electrons are produced within the DNA by either direct ionization or indirect ionization via hole and electron transfer from the surrounding water to DNA.[23] Due to the relatively

(1) Löwdin, P. O. *Rev. Mod. Phys.* **1963**, *35*, 724.
(2) Löwdin, P. O. *Adv. Quantum Chem.* **1965**, *2*, 213.
(3) Dąbkowska, I.; Rak, J.; Gutowski, M. *Eur. Phys. J. D* **2005**, *35*, 429.
(4) Gu, J.; Wang, J.; Rak, J.; Leszczynski, J. *Angew. Chem., Int. Ed.* **2007**, *46*, 3479.
(5) Sobolewski, A. L.; Domcke, W. *Phys. Chem. Chem. Phys.* **2004**, *6*, 2763.
(6) Sobolewski, A. L.; Domcke, W.; Hättig, C. *Proc. Natl. Acad. Sci. U.S.A.* **2005**, *102*, 17903.
(7) Perun, S.; Sobolewski, A. L.; Domcke, W. *J. Phys. Chem. A* **2006**, *110*, 9031.
(8) Schwalb, N. K.; Temps, F. *J. Am. Chem. Soc.* **2007**, *129*, 9272.
(9) Wagenknecht, H. A. *Angew. Chem., Int. Ed.* **2003**, *42*, 2454.
(10) Ito, T.; Rokita, S. E. *Angew. Chem., Int. Ed.* **2004**, *43*, 1839.
(11) Ghosh, A. K.; Schuster, G. B. *J. Am. Chem. Soc.* **2006**, *128*, 4172.
(12) Florián, J.; Leszczyñski, J. *J. Am. Chem. Soc.* **1996**, *118*, 3010.
(13) Gorb, L.; Podolyan, Y.; Dziekonski, P.; Sokalski, W. A.; Leszczyński, J. *J. Am. Chem. Soc.* **2004**, *126*, 10119.
(14) Villani, G. *Chem. Phys.* **2006**, *324*, 438.
(15) Villani, G. *Chem. Phys.* **2005**, *316*, 1.
(16) Noguera, M.; Sodupe, M.; Bertrán, J. *Theor. Chem. Acc.* **2007**, *118*, 113.
(17) Guallar, V.; Douhal, A.; Moreno, M.; Lluch, J. M. *J. Phys. Chem. A* **1999**, *103*, 6251.
(18) Bertrán, J.; Oliva, A.; Rodríguez-Santiago, L.; Sodupe, M. *J. Am. Chem. Soc.* **1998**, *120*, 8159.
(19) Li, X.; Cai, Z.; Sevilla, M. D. *J. Phys. Chem. B* **2001**, *105*, 10115.
(20) Chen, H. Y.; Chao, I. *ChemPhysChem* **2004**, *5*, 1855.
(21) Radisic, D.; Bowen, K. H.; Dabkowska, I.; Storoniak, P.; Rak, J.; Gutowski, M. *J. Am. Chem. Soc.* **2005**, *127*, 6443.
(22) Szyperska, A.; Rak, J.; Leszczynski, J.; Li, X.; Ko, Y. J.; Wang, H.; Bowen, K. H. *J. Am. Chem. Soc.* **2009**, *131*, 2663.
(23) Cai, Z.; Sevilla, M. D. *Top. Curr. Chem.* **2004**, *237*, 103.

10.1021/ja906899p CCC: $40.75

low ionization potential of guanine (G), positive holes eventually migrate to and localize on the G sites; on the other hand, electrons can occupy both thymine (T) and cytosine (C) sites because they have comparable electron affinities.[24−27] The pK_a value for N3 proton of protonated electron adduct C(N3+H)$^{\bullet}$ (p$K_a > 13$) was measured to be significantly larger than that of N1 proton of neutral G (p$K_a = 9.5$),[28] and the pK_a of N1 proton of oxidized G$^{\bullet+}$ (p$K_a = 3.9$) was measured to be slightly smaller than the pK_a of N3-protonated C(N3+H)$^+$ cation (pK_a = 4.3).[29,30] These pK_a data of isolated nucleobases imply that both excess electron on C and positive hole on G would induce a proton transfer from N1 of G to N3 of C in G:C base pairs. In contrast, analogous proton transfer in the adenine−thymine (A:T) base pair was inferred to be energetically unfavorable based on the pK_a measurements.[28,30] The density functional theory (DFT) calculations on the isolated G:C base pair have confirmed that the proton-transfer reaction in G:C$^{\bullet-}$ is exothermic by ca. 3 kcal/mol with a small barrier of ca. 1 kcal/mol; however, the proton transfer was predicted to be slightly endothermic by ca. 1.4 kcal/mol with a moderate barrier of ca. 3 kcal/mol in G$^{\bullet+}$:C, in contrast to the pK_a measurements.[19] The proton-transfer reaction in the 2′-deoxyriboguanosine-2′-deoxyribocytidine nucleoside pair radical anion has also been investigated by DFT calculations; the results showed that the sugar moiety has almost no effect on the proton-transfer reaction.[31] Very recently, Bowen and co-workers performed a joint computational and photoelectron spectroscopy study for the radical anion of 9-methylguanine-1-methylcytosine (mG:mC).[22] Their calculations for the neutral mG:mC indicated that the Watson−Crick configuration is substantially more stable than other hydrogen-bonding patterns and is, therefore, dominant in gas-phase mixtures. Further, they found that the photoelectron spectrum for the radical anion of mG:mC, which displays a broad peak at an unexpectedly high-energy region of ∼2.1 eV, can only be accounted for by the electron vertical detachment energy of the proton-transferred form, mG(N1−H)$^-$:mC(N3+H)$^{\bullet}$, of the Watson−Crick base pair. The work of Bowen et al. provides solid evidence that electron addition on the isolated G:C base pair indeed triggers the proton shift along the middle hydrogen bond.

The proton transfer from G$^{\bullet+}$ to complementary C has also been observed in double-stranded DNA in nanosecond pulse radiolysis experiments. By monitoring the absorbance increase at 625 nm, which is the characteristic absorption of deprotonated neutral radical, G(N1−H)$^{\bullet}$, the deprotonation of G$^{\bullet+}$ within the DNA duplex was estimated to occur in the time scale of microseconds.[32,33] Similar experiment has been carried out to record the transient spectra of G:C and A:T base-pair radical anions in duplex DNA.[34] The absorbance change for A:T$^{\bullet-}$ in the microsecond time scale was clearly observed and attributed to the irreversible protonation on the C6 site of T$^{\bullet-}$. In contrast, no such spectrum change was detected for G:C$^{\bullet-}$. On the basis of the pK_a data mentioned above, the authors inferred that the proton transfer in G:C$^{\bullet-}$ is complete within 10 ns (the pulse width used in that work) and regarded the observed spectrum as the signature of the proton-transferred structure, G(N1−H)$^-$:C(N3+H)$^{\bullet}$. The presence of deuterium isotope effect on the efficiency of charge transfer in duplex DNA provides additional evidence for the intra-base-pair proton transfer induced by ionization.[35−38]

The proton transfer in reduced and oxidized G:C base pairs is considered to be relevant to two currently hot research topics, namely, charge transport along DNA and low-energy electron (LEE)-induced DNA damage. For example, this concept has been invoked to explain why the excess electron transfer along G:C stacks is less efficient than that along A:T stacks.[9,10] In addition, it has been proposed that the proton-transferred structure, G(N1−H)$^-$:C(N3+H)$^{\bullet}$, can capture a second excess electron to form a stable dianion, G(N1−H)$^-$:C(N3+H)$^-$, which subsequently triggers the cleavage of either a sugar−phosphate bond or a glycosidic bond.[3,4]

To get insights into the behaviors of ionized base pairs buried in DNA under physiological conditions, the effects of external interactions experienced by embedded base pairs have to be considered. Previous theoretical studies have demonstrated profound influences of base stacking on ionization potentials[39,40] and electron affinities of nucleobases[41,42] and on energetic barriers of sugar−phosphate bond breaking induced by LEEs.[43,44] Recently, a joint electron spin resonance (ESR) and DFT study pointed out that A$^{\bullet+}$ in adenine stacks displays very dissimilar acid−base properties (i.e., different pK_a values) from isolated A$^{\bullet+}$.[45] The theoretical studies concerning the environmental effects on the proton-transfer reaction in ionized base pairs, although scarce, have also appeared. Large-scale quantum mechanics/molecular mechanics (QM/MM) simulations predicted the preference for the protonation state of G(N1−H)$^{\bullet}$:C(N3+H)$^+$ rather than the canonical G$^{\bullet+}$:C in a fully hydrated DNA duplex,[46] contrary to the computational result of isolated base pair.[19] A recent DFT study has shown that the reverse stability of the protonation state of the oxidized G:C base pair is originated from the hydration effect with most of the influence coming from the first hydration shell.[47]

In the present work, we report a comprehensive computational study on the proton-transfer reaction in G:C$^{\bullet-}$ embedded in duplex DNA, which takes the interactions of base stacking, sugar−phosphate backbone, counterions, as well as hydration

(24) Seidel, C. A. M.; Schulz, A.; Sauer, M. H. M. *J. Phys. Chem.* **1996**, *100*, 5541.
(25) Steenken, S.; Jovanovic, S. V. *J. Am. Chem. Soc.* **1997**, *119*, 617.
(26) Li, X.; Cai, Z.; Sevilla, M. D. *J. Phys. Chem. A* **2002**, *106*, 9345.
(27) Giese, B. *Annu. Rev. Biochem.* **2002**, *71*, 51.
(28) Steenken, S.; Telo, J. P.; Novais, H. M.; Candeias, L. P. J. *J. Am. Chem. Soc.* **1992**, *114*, 4701.
(29) Candeias, L. P.; Steenken, S. *J. Am. Chem. Soc.* **1989**, *111*, 1094.
(30) Steenken, S. *Chem. Rev.* **1989**, *89*, 503.
(31) Gu, J.; Xie, Y.; Schaefer, H. F. *J. Chem. Phys.* **2007**, *127*, 155107.
(32) Kobayashi, K.; Tagawa, S. *J. Am. Chem. Soc.* **2003**, *125*, 10213.
(33) Kobayashi, K.; Yamagami, R.; Tagawa, S. *J. Phys. Chem. B* **2008**, *112*, 10752.
(34) Yamagami, R.; Kobayashi, K.; Tagawa, S. *J. Am. Chem. Soc.* **2008**, *130*, 14772.
(35) Shafirovich, V.; Dourandin, A.; Geacintov, N. E. *J. Phys. Chem. B* **2001**, *105*, 8431.
(36) Weatherly, S. C.; Yang, I. V.; Thorp, H. H. *J. Am. Chem. Soc.* **2001**, *123*, 1236.
(37) Giese, B.; Wessely, S. *Chem. Commun.* **2001**, 2108.
(38) Cai, Z.; Gu, Z.; Sevilla, M. D. *J. Phys. Chem. B* **2000**, *104*, 10406.
(39) Sugiyama, H.; Saito, I. *J. Am. Chem. Soc.* **1996**, *118*, 7063.
(40) Prat, F.; Houk, K. N.; Foote, C. S. *J. Am. Chem. Soc.* **1998**, *120*, 845.
(41) Voityuk, A. A.; Michel-Beyerle, M. E.; Rösch, N. *Chem. Phys. Lett.* **2001**, *342*, 231.
(42) Kobylecka, M.; Leszczynski, J.; Rak, J. *J. Am. Chem. Soc.* **2008**, *130*, 15683.
(43) Simons, J. *Acc. Chem. Res.* **2006**, *39*, 772.
(44) Anusiewicz, I.; Berdys, J.; Sobczyk, M.; Skurski, P.; Simons, J. *J. Phys. Chem A* **2004**, *108*, 11381.
(45) Adhikary, A.; Kumar, A.; Khanduri, D.; Sevilla, M. D. *J. Am. Chem. Soc.* **2008**, *130*, 10282.
(46) Gervasio, F. L.; Laio, A.; Iannuzzi, M.; Parrinello, M. *Chem.−Eur. J.* **2004**, *10*, 4846.
(47) Kumar, A.; Sevilla, M. D. *J. Phys. Chem. B* **2009**, *113*, 11359.

into account. By constructing molecular models that consist of different components of DNA and comparing the results between them, the above-mentioned interactions were individually separated and analyzed. The results showed that the backbone and counterions have minor effects, but the base stacking and hydration have important effects on the proton transfer in G:C$^{\bullet-}$. The effect of G:C stacking was proven to be electrostatic in nature and tends to retard the proton-transfer reaction. In contrast, the hydration was found to significantly facilitate the proton transfer. On the basis of the present findings, the effect of base sequence was also predicted. We also examined the possibility of accommodating two excess electrons in a G:C base pair buried in DNA duplex. The correlations between our computational results and experiments are discussed, and the implications of our findings to many issues are given.

2. Computational Methods

The double-stranded B-form DNA trimer, d(5′-GGG-3′)·d(3′-CCC-5′), which is hereafter denoted as $(dG:dC)_3$, was constructed by the nucleic acid database in the HyperChem package.[48] The phosphate groups were terminated by hydrogen atoms to simulate the condition of DNA with close-contact counterions. To separate the influences of backbone and base stacking, the model of the base-pair trimer, $(G:C)_3$, was obtained by deleting the sugar−phosphate backbone from $(dG:dC)_3$ and completing the valence by hydrogenation. Since the size of molecular systems under investigation is large and the electronic state concerned is an open shell that should be treated with unrestricted SCF calculations, the computational cost is unaffordable for full geometry optimization with full DFT description. To make the calculations feasible, a two-layer ONIOM approach developed by Morokuma's group[49] was adopted and the geometry optimizations and relaxed potential energy surface (PES) scans were performed in a partial optimization scheme. In these calculations, the middle G:C base pairs in $(G:C)_3^{\bullet-}$ and $(dG:dC)_3^{\bullet-}$ were treated by the DFT B3LYP/6-31+G* method and allowed for geometry relaxation (the fragments rendered by ball-and-stick in Figure 1), whereas the remaining parts, including the peripheral base pairs and the sugar−phosphate backbone, were described by semiempirical PM3 method and fixed in geometry (the fragments rendered by wireframe in Figure 1). For $(G:C)_3^{\bullet-}$, the coordinates of hydrogen atoms connected to N9 of middle G and N1 of middle C were also fixed during the geometry optimizations and PES scans to prevent irrelevant geometry relaxation of the middle base pair, such as lateral displacement to escape from the π-stack.

Partial geometry optimizations were first performed to find the canonical Watson−Crick (WC) structure, in which the proton is connected to N1 of G, and the proton-transferred (PT) structure, in which the proton is connected to N3 of C, for $(G:C)_3^{\bullet-}$ and $(dG:dC)_3^{\bullet-}$. Then the calculations of the partially relaxed PES scan starting from WC to PT structures with increasing N1(G)−H bond length were carried out to locate the transition-state (TS) structure for the proton-transfer reaction. Full B3LYP/6-31+G* single-point energy calculations were performed for selected ONIOM(B3LYP/6-31+G*:PM3) structures to obtain more accurate B3LYP/6-31+G*//ONIOM(B3LYP/6-31+G*:PM3) PESs for the proton transfer in $(G:C)_3^{\bullet-}$ and $(dG:dC)_3^{\bullet-}$. Additional single-point energy calculations using recently developed M05-2X[50a,c] and M06-2X functionals[50b,c] were also carried out to verify the reliability of the B3LYP results. For comparison, the corresponding partial geometry optimizations and partially relaxed PES scan for the isolated G:C base-pair radical anion were also performed; the geometric constraint, namely, the frozen H atoms connected to N9 of G and N1 of C, makes the proton-transfer barrier somewhat higher (4.7 vs 3.6 kcal/mol) and the proton-transfer energy somewhat lower (−3.9 vs −3.0 kcal/mol) relative to the previous results of full geometry optimizations.[19] Most of the calculations were performed by Gaussian 03 package,[51] except those of the M06-2X calculations, which were achieved with Jaguar code.[52]

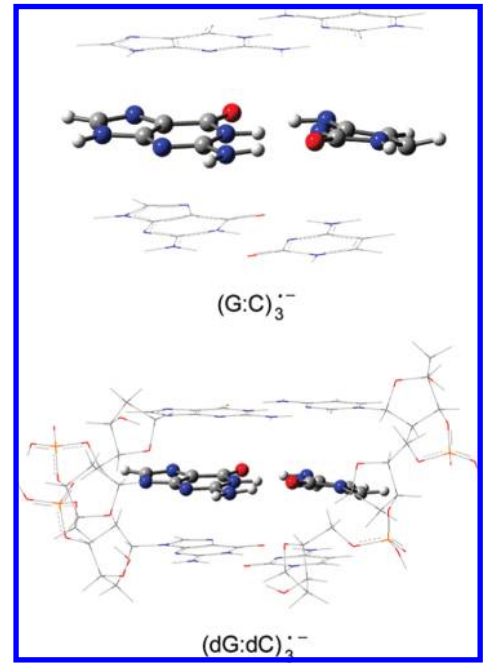

Figure 1. ONIOM layer definition for $(G:C)_3^{\bullet-}$ and $(dG:dC)_3^{\bullet-}$. The ball-and-stick representation denotes high-level layer treated by B3LYP/6-31+G* method, and the wireframe representation denotes low-level layer treated by PM3 method.

The proton-transfer rates were roughly evaluated by the equation

$$k_{pt} = \nu \exp(-E^*/RT)$$

where ν is the vibrational frequency of the N−H bond and E^* is the activation energy for the proton-transfer reaction. Here, the N−H vibrational frequency was approximated by 3000 cm^{-1}. Since the zero-point-energy (ZPE) corrections for partially optimized structures are meaningless and not available, we instead assumed the value of −2.6 kcal/mol, which was derived from the frequency calculations for the fully optimized structures of isolated G:C$^{\bullet-}$ at the B3LYP/6-31+G* level, for the ZPE corrections on the proton-transfer barriers.

3. Results

3.1. Environmental Effects. Figure 2 presents a comparison of potential energy surfaces for the proton transfer from N1 of G to N3 of C in the isolated G:C$^{\bullet-}$ base pair, $(G:C)_3^{\bullet-}$ base-

(48) *HyperChem Professional 8.0.3*; Hypercube, Inc., 1115 NW 4th Street, Gainesville, FL 32601.

(49) (a) Maseras, F.; Morokuma, K. *J. Comput. Chem.* **1995**, *16*, 1170. (b) Humbel, S.; Sieber, S.; Morokuma, K. *J. Chem. Phys.* **1996**, *105*, 1959. (c) Matsubara, T.; Sieber, S.; Morokuma, K. *Int. J. Quantum Chem.* **1996**, *60*, 1101. (d) Svensson, M.; Humbel, S.; Froese, R. D. J.; Matsubara, T.; Sieber, S.; Morokuma, K. *J. Phys. Chem.* **1996**, *100*, 19357. (e) Svensson, M.; Humbel, S.; Morokuma, K. *J. Chem. Phys.* **1996**, *105*, 3654. (f) Dapprich, S.; Komáromi, I.; Byun, K. S.; Morokuma, K.; Frisch, M. J. *J. Mol. Struct. (THEOCHEM)* **1999**, *462*, 1. (g) Vreven, T.; Morokuma, K. *J. Comput. Chem.* **2000**, *21*, 1419.

(50) (a) Zhao, Y.; Schultz, N. E.; Truhlar, D. G. *J. Chem. Theory Comput.* **2006**, *2*, 364. (b) Zhao, Y.; Truhlar, D. G. *Theor. Chem. Acc.* **2008**, *119*, 525. (c) Zhao, Y.; Truhlar, D. G. *Acc. Chem. Res.* **2008**, *41*, 157.

(51) Frisch, M. J. *GAUSSIAN 03*, revision E.01; Gaussian, Inc.: Wallingford, CT, 2004.

(52) *Jaguar*, version 7.5; Schrödinger, LLC: New York, 2008.

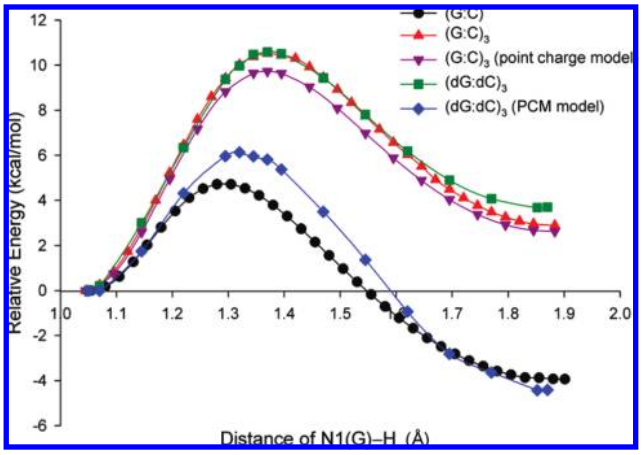

Figure 2. B3LYP/6-31+G*//ONIOM(B3LYP/6-31+G*:PM3) potential energy surfaces for the proton transfer from N1 of guanine to N3 of cytosine induced by electron attachment.

Table 1. B3LYP/6-31+G* Results of Activation Energies, Reaction Energies, Rate Constants, and Equilibrium Constants for the Proton-Transfer Reaction in Guanine−Cytosine Base-Pair Radical Anion in Different Models[a]

model	E^* (kcal/mol)[b]	E_{rxn} (kcal/mol)	k_{pt} (s^{-1})	K_{eq}
$(G:C)^{\bullet-}$	4.7 (2.1)	−3.9	2.6×10^{12}	7.2×10^{2}
$(G:C)_3^{\bullet-}$	10.5 (7.9)	2.9	1.4×10^{8}	7.5×10^{-3}
$(dG:dC)_3^{\bullet-}$	10.6 (8.0)	3.7	1.2×10^{8}	1.9×10^{-3}
$(dG:dC)_3^{\bullet-}$ + PCM	6.0 (3.4)	−4.4	2.9×10^{11}	1.7×10^{3}
$(dG:dC)_3^{\bullet-}\cdot 5H_2O$	6.3 (3.7)	−3.1	1.7×10^{11}	1.9×10^{2}
$(dG:dC)_3^{\bullet-}\cdot 5H_2O$ + PCM	5.4 (2.8)	−5.9	8.0×10^{11}	2.1×10^{4}
$(dG:dC)_3^{\bullet-5}$	11.6 (9.0)	6.6	2.3×10^{7}	1.4×10^{-5}
$(dG:dC)_3^{\bullet-5}$ + PCM	5.6 (3.0)	−4.5	5.7×10^{11}	2.0×10^{3}

[a] Rate constants and equilibrium constants are estimated at 298 K. [b] The values in parentheses are ZPE-corrected activation energies. The ZPE corrections for different models are assumed to be the same (−2.6 kcal/mol) and are derived from the frequency calculations for the fully optimized structures of isolated guanine−cytosine base-pair radical anion.

pair trimer, and $(dG:dC)_3^{\bullet-}$ DNA trimer. For clarity, only full DFT results of B3LYP/6-31+G*//ONIOM(B3LYP/6-31+G*:PM3) are shown in Figure 2. The corresponding ONIOM(B3LYP/6-31+G*:PM3) PESs are given in Supporting Information. The activation energies and reaction energies of the proton transfer in different models are collected in Table 1.

3.1.1. Base Stacking Effect. A comparison between the results of $G:C^{\bullet-}$ and $(G:C)_3^{\bullet-}$ in Figure 2 clearly shows that base stacking has a pronounced effect on the proton transfer in $G:C^{\bullet-}$. The proton-transfer reaction, which is exothermic in isolated $G:C^{\bullet-}$, becomes endothermic with considerably enhanced barrier in $(G:C)_3^{\bullet-}$; the activation energy increases from 4.7 to 10.5 kcal/mol, and the reaction energy increases from −3.9 to 2.9 kcal/mol upon G:C stacking (Table 1).

An interesting and important question thus naturally emerges, namely, what is the physical origin of the G:C stacking effect? One of the possibilities is delocalization of excess electron within G:C stacks, which is expected to attenuate the basicity increasing on the N3 of C caused by electron attachment, and thereby makes the proton transfer less easier to proceed compared to the isolated $G:C^{\bullet-}$. However, the natural population analysis (NPA) of charge and spin distributions in $(G:C)_3^{\bullet-}$ apparently disagrees with this argument. The analysis reveals that more than 90% of the excess negative charge and spin are localized on the middle base pair during the proton-transfer process (Table 2). The profiles of singly occupied molecular orbitals (SOMOs) for $(G:C)_3^{\bullet-}$, which are largely confined to the middle C, are in line with the NPA analyses (Figure 3). The localization of positive hole or excess electron on an individual base in base or base-pair stacks has been reported in many cases.[39,41,42,53] One exception is the positive hole in adenine stacks.[45] The propensity toward delocalization of the positive hole in adenine stacks was attributed to an unusually small geometric change (i.e., small reorganization energy) for the formation of adenine cation.[45]

Table 2. Natural Population Analysis of Charge and Spin on the Middle G:C Base Pair in $(G:C)_3^{\bullet-}$ at Canonical Watson−Crick, Transition-State, and Proton-Transferred Structures

	WC			TS			PT		
	G	C	total	G	C	total	G	C	total
charge	−0.09	−0.82	−0.91	−0.71	−0.24	−0.95	−0.86	−0.11	−0.97
spin	0.00	0.90	0.90	0.00	0.94	0.94	0.00	0.97	0.97

An alternative origin of the base stacking effect might be electrostatic interaction. We noticed that a neutral G:C base pair possesses a remarkably large dipole moment (∼6 D) with the negative end on G and the positive end on C. In $(G:C)_3^{\bullet-}$, the arrangements of dipole moments for top and bottom G:C base pairs thereby tend to stabilize the canonical WC structure (i.e., reactant), where the majority of excess negative charge is localized on the middle C, and tend to destabilize the TS and PT (i.e., product) structures, where most of the negative charge

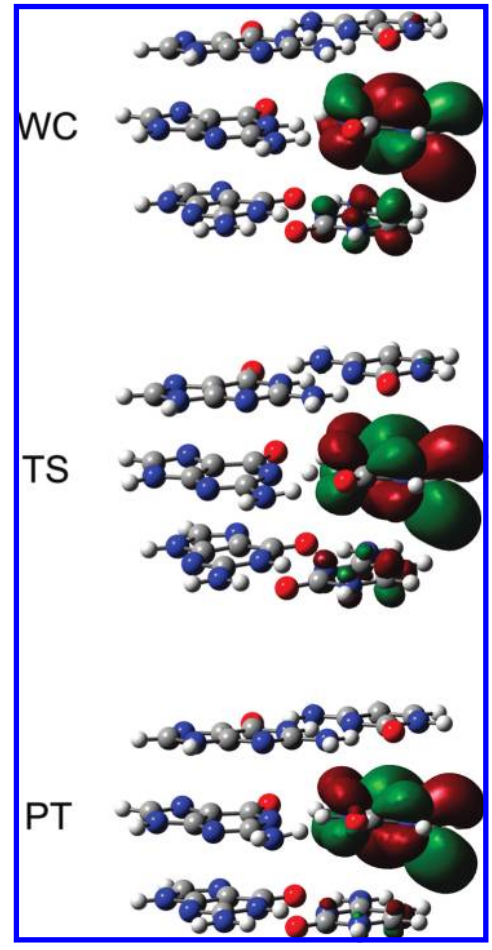

Figure 3. Singly occupied molecular orbitals of $(G:C)_3^{\bullet-}$ at canonical Watson−Crick, transition-state, and proton-transferred structures.

is shifted onto the middle G (Table 2). These effects collectively raise the kinetic barrier and reaction energy for the proton-transfer reaction. To verify this argument, we recalculated the PES for the proton transfer in $(G:C)_3^{\bullet-}$ by replacing the outer G:C base pairs by atomic point charges derived from CHELPG scheme to reproduce the dipole moment of neutral G:C base pair. In these calculations, the charge delocalization among base pairs is totally excluded, and only electrostatic interaction is taken into account. The resultant PES for the fictitious $(G:C)_3^{\bullet-}$ is very close to that for the complete $(G:C)_3^{\bullet-}$ (Figure 2), definitely certifying that electrostatic interaction is responsible for the G:C stacking effect on the proton-transfer reaction. The deviation between the two PESs, which can be ascribed to the charge-delocalization effect, is minor and negligible, consistent with the localization nature of excess electron revealed by NPA and SOMO analyses.

3.1.2. Backbone and Counterion Effects. The calculated activation energy and reaction energy for the proton transfer in DNA trimer $(dG:dC)_3^{\bullet-}$, which includes the sugar−phosphate backbone with hydrogenations on phosphate groups, are very close to the values in base-pair trimer $(G:C)_3^{\bullet-}$, indicating that the backbone has negligible effect on the proton-transfer reaction (Figure 2 and Table 1). This result is consistent with and can be regarded as an extension of the previous theoretical study of the 2′-deoxyriboguanosine-2′-deoxyribocytidine nucleoside pair radical anion, in which the sugar moiety was found to affect the proton transfer very little.[31]

To explore the counterion effect, we took off the hydrogen atoms originally added on the phosphate groups and recalculated the proton-transfer barrier and energy. In this molecular model, the DNA trimer bears five negative charges and is denoted as $(dG:dC)_3^{\bullet-5}$. The activation energy slightly increases from 10.6 to 11.6 kcal/mol, and the reaction energy moderately increases from 3.7 to 6.6 kcal/mol when going from $(dG:dC)_3^{\bullet-}$ to $(dG:dC)_3^{\bullet-5}$ (Table 1). The influence of counterions, while not completely negligible, is relatively minor in comparison to the influence of base stacking. In addition, it will be seen later that the counterion effect is further reduced upon hydration.

3.1.3. Hydration Effect. In order to simulate the hydration environment of DNA, polarizable continuum model (PCM) was applied to $(dG:dC)_3^{\bullet-}$. It was found that the hydration significantly assists the proton-transfer reaction; the barrier is reduced to 6 kcal/mol, and the reaction becomes exothermic by 4.4 kcal/mol upon hydration (Table 1). The influence of hydration can be rationalized by the existence of more electronegative atoms which are exposed to DNA grooves and can be approached by water on G (N3, O6, and N7 atoms) than on C (O2 atom), as a result, favoring the water polarization to stabilize the negative charge on G (i.e., TS and PT structures) rather than on C (i.e., WC structure).

We also incorporated the effect of explicit water. To do so, five water molecules described at the B3LYP/6-31+G* level were initially put around the N3(G), O6(G), N7(G), O2(C), and N4(C) sites of the middle base pair in a normal hydrogen-bonding pattern; the initial positions of water molecules were chosen according to the hydration sites (occupancy >0.5) determined by a previous analysis of 14 B-DNA crystal structures.[54] The coordinates of water molecules were then optimized under the conditions that the geometry of remaining $(dG:dC)_3^{\bullet-}$ was fixed at gas-phase WC, TS, and PT structures. The additional effect of bulk solvation was incorporated by applying PCM calculations on the $(dG:dC)_3^{\bullet-}\cdot 5H_2O$. It is evident from the data in Table 1 that the majority of the hydration effect comes from the first hydration shell; the inclusion of bulk hydration by the PCM model further lowers the barrier and reaction energy of the proton transfer but only has a minor effect. Despite the fact that the proton-transfer activation energies and reaction energies derived from the three models, $(dG:dC)_3^{\bullet-}$ + PCM, $(dG:dC)_3^{\bullet-}\cdot 5H_2O$, and $(dG:dC)_3^{\bullet-}\cdot 5H_2O$ + PCM, are somewhat different, all of these calculations lead to the same conclusion; that is, hydration substantially facilitates the proton transfer in buried $G:C^{\bullet-}$. The results that hydration tends to favor the proton transfer and the important role played by the first hydration shell have been reported for the isolated $G^{\bullet+}$:C base-pair radical cation.[47] It is interesting to notice that the hydration effect for $(dG:dC)_3^{\bullet-}$ observed in the present study is remarkably larger than that for $G^{\bullet+}$:C predicted previously. Moreover, the comparison between the results of $(dG:dC)_3^{\bullet-}$ + PCM and $(dG:dC)_3^{\bullet-}\cdot 5H_2O$ + PCM demonstrates that the PCM model can qualitatively and even semiquantitatively characterize the hydration effect on the proton transfer in $G:C^{\bullet-}$ (Table 1).

We also carried out PCM calculations on the DNA trimer without counterions (i.e., no hydrogenations on phosphate groups). The calculations show that there is almost no difference in the proton-transfer energetics for $(dG:dC)_3^{\bullet-}$ + PCM and $(dG:dC)_3^{-5}$ + PCM models (Table 1). This means that the influences of negative charges on phosphate groups are almost completely screened out by bulk solvation. In other words, the behavior of the proton transfer in reduced DNA should be nearly independent of the presence of counterions in aqueous environment. The similar screening effect of solvation on electron affinities of nucleotides has been reported, as well.[55]

3.2. Can G:C Capture Two Excess Electrons? As mentioned in the Introduction, the formation of base-pair dianions might be in connection with the DNA damages caused by LEEs. To examine the possibility of accommodation of two excess electrons on a single base pair in DNA, the adiabatic electron affinity (AEA) of the proton-transferred structure of $(dG:dC)_3^{\bullet-}$ was evaluated by the energy difference between the monoanion and dianion at their corresponding optimized geometries. The resultant AEA was found to be highly negative (−2.136 eV) without considering any hydration effect, indicating that the dianion of $G(N1-H)^-:C(N3+H)^-$ is unstable against electron autodetachment, the process that is expected to occur in the time scale of 10^{-14} s. The inclusion of five water molecules around the middle base pair, although increased the AEA to −1.880 eV, did not make the dianion stable. However, the AEA of $(dG:dC)_3^{\bullet-}$ turned into a positive value of 1.077 eV when the bulk hydration was incorporated using the PCM model. Our calculations thus predict that the $G(N1-H)^-:C(N3+H)^-$ base-pair dianion in the DNA duplex is not stable in dry conditions that contain only structural water, but they are indeed stable in aqueous solution.

3.3. M05-2X and M06-2X Results. It is well-known that B3LYP method has a weakness in describing a $\pi-\pi$ stacking interaction that is dominated by medium-range electron-correlation energy.[50] To test the reliability of the B3LYP results mentioned above, additional calculations using recently developed M05-2X[50a,c] and M06-2X[50b,c] functionals, which were especially designed to improve $\pi-\pi$ stacking interaction, were

(53) Blancafort, L.; Voityuk, A. A. *J. Phys. Chem. A* **2007**, *111*, 4714.
(54) Schneider, B.; Berman, H. M. *Biophys. J.* **1995**, *69*, 2661.
(55) Gu, J.; Xie, Y.; Schaefer, H. F. *ChemPhysChem* **2006**, *7*, 1885.

performed to reinvestigate the base stacking effect on the proton transfer in $(G:C)_3^{\bullet-}$. The activation energy and reaction energy evaluated by M05-2X/6-31+G* (10.1 and 2.1 kcal/mol) and M06-2X/6-31+G* (9.2 and 2.1 kcal/mol) single-point energy calculations on ONIOM(B3LYP/6-31+G*:PM3) optimized structures are very close to those obtained by B3LYP/6-31+G* calculations (10.5 and 2.9 kcal/mol). In addition, the charge and spin distributions of $(G:C)_3^{\bullet-}$ predicted by the three functionals are also similar. This infers that the dispersion interaction, which plays an essential role in aromatic−aromatic binding, appears to have negligible influence on the intra-base-pair proton transfer, in accord with our previous analysis that the electrostatic interaction is responsible for the G:C stacking effect on the proton-transfer reaction.

4. Discussion

Using the present energetic data, the proton-transfer rates at 298 K for $(dG:dC)_3^{\bullet-}$ in gas phase and in aqueous solution were roughly estimated to be 10^8 and 8×10^{11} s^{-1}, respectively (Table 1). Moreover, the equilibrium constants in the two circumstances were predicted to differ by 7 orders of magnitude ($K_{eq} \sim 10^{-3}$ in gas phase and $\sim 10^4$ in water). The rate of the proton transfer within $G:C^{\bullet-}$ should be compared with the rate of excess electron transfer between neighboring G:C base pairs. The hopping rate of positive hole from G to GG across a single A was measured to be 10^7 s^{-1}.[56] Furthermore, the hole transfer between adjacent adenines was determined to be 2×10^{10} s^{-1}.[57] While the rate of excess electron transfer in DNA has not been directly measured yet, recent studies have pointed out that both electron and hole transfer along DNA display similar characteristics.[58,59] On the basis of the assumption that the excess electron transfer between adjacent cytosines is as fast as hole transfer ($\sim 10^{10}$ s^{-1}), the present results suggest that the proton transfer within $G:C^{\bullet-}$ can efficiently interfere with the electron transfer along G:C stacks in wet conditions that include at least the water molecules in the first hydration layer but not in extremely dry conditions. This theoretical prediction might have connections with some of the experimental results. For example, ESR study of irradiated DNA at 77 K has revealed that the rate and distance of electron transfer along the DNA duplex slightly decrease as the hydration level increases,[60] consistent with our prediction that the hydration favors the intra-base-pair proton transfer, which, in turn, leads to electron trapping in the charge-spin-separated form $G(N1-H)^-:C(N3+H)^{\bullet}$. Someone may consider this experimental observation to be probably associated with the conformational changes of DNA caused by different degrees of hydration. It is well-established that DNA adopts the B-form in the conditions of high humidity (>13 H_2O/nucleotide) but exists in the A-form in the conditions of low humidity. Although the A-DNA is characterized by a more compact helical structure (base-pair separation of 2.4 Å and twist angle of 32.7°) in comparison to the B-DNA (base-pair separation of 3.4 Å and twist angle of 36°), the former, nevertheless, displays poorer effective π-orbital overlap between neighboring base pairs than the latter, as demonstrated by the electronic coupling calculations.[61] From this point of view, the electron transfer along DNA is expected to be more efficient in wet conditions rather than in dry conditions, which obviously conflicts with the experimental results. Accordingly, it appears that the hydration-level dependence of electron-transfer rate and distance along DNA cannot be rationalized by the conformational changes induced by hydration. Our results also explain the experimental measurements of radical composition for irradiated DNA, which showed that the $T^{\bullet-}$ radical dominates at low hydration, whereas the $C(N3+H)^{\bullet}$ radical overcomes at higher hydration.[62]

In 2000, Boudaïffa et al. exposed DNA thin film to LEEs in the range of 3−20 eV and found the occurrence of single- and double-strand breaks (SSBs and DSBs).[63] A later experiment further showed that electrons with even lower energies (0−4 eV) can also lead to SSBs.[64] These pioneering experimental works inspired extensive theoretical investigations on the mechanism of DNA damage induced by LEEs.[3,43,44,65−69] One of the possible pathways is that the LEEs first attach to the π^* orbitals of nucleobases and the subsequent strand breaks are accompanied and promoted by an excess electron transfer from π^* on bases to σ^* on the sugar−phosphate backbone.[43,44,65,66] Recent DFT calculations of cytosine nucleotides predicted the ZPE-corrected barrier of 4.68 and 12.52 kcal/mol for C3′−O and C5′−O bond cleavages, respectively, indicating that the LEE-induced SSB of DNA chiefly occurs on the C3′−O bond.[65,66] The remarkably lower barrier for the C3′−O bond rupture can be understood by a process analogous to the S_N2 reaction where the attack on C3′ from the opposite side of the leaving phosphate group by the excess electron on nucleobase is directly and easily achieved.[66] In contrast, such an attack is forbidden in the 5′-monophosphate nucleotide due to the steric reason. In addition, the hydration was found to increase the activation energy of C3′−O bond cleavage by 6.65 kcal/mol.[66] Using the method that we previously evaluated the proton-transfer rate and assuming the stretching frequency of 1000 cm^{-1} for C−O bond, the C3′−O bond-cleavage rates were estimated to be ca. 10^5 and 10^{10} s^{-1} in the condition with and without hydration, respectively. A similar maximum rate of sugar−phosphate bond cleavage in the gas phase has also been reported by previous ab initio Hartree−Fock studies.[43] These data, in combination with the present results, reveal that the mechanism of LEE-induced DNA damage is highly susceptible to the degree of hydration. In the condition without water, electron attachment to the π^* orbital of cytosine can efficiently trigger the SSB of DNA via the electron transfer to the σ^* orbital on sugar−phosphate backbone ($\sim 10^{10}$ s^{-1}). As the hydration level slightly increases to the extent that the first hydration shell around the base pair is filled, the proton transfer within the $G:C^{\bullet-}$ ($\sim 10^{11}$ s^{-1}) starts to overcome the electron transfer from π^* to σ^*, which slows down upon hydration ($\sim 10^5$ s^{-1}), and the SSB is

(56) Lewis, F. D.; Liu, X.; Liu, J.; Miller, S. E.; Hayes, R. T.; Wasielewski, M. R. *Nature* **2000**, *406*, 51.
(57) Takada, T.; Kawai, K.; Cai, X.; Sugimoto, A.; Fujitsuka, M.; Majima, T. *J. Am. Chem. Soc.* **2004**, *126*, 1125.
(58) Valis, L.; Wang, Q.; Raytchev, M.; Buchvarov, I.; Wagenknecht, H. A.; Fiebig, T. *Proc. Natl. Acad. Sci. U.S.A.* **2006**, *103*, 10192.
(59) Elias, B.; Shao, F.; Barton, J. K. *J. Am. Chem. Soc.* **2008**, *130*, 1152.
(60) Cai, Z.; Gu, Z.; Sevilla, M. D. *J. Phys. Chem. B* **2001**, *105*, 6031.
(61) Endres, R. G.; Cox, D. L.; Singh, R. R. P. *Rev. Mod. Phys.* **2004**, *76*, 195.
(62) Wang, W.; Yan, M.; Becker, D.; Sevilla, M. D. *Radiat. Res.* **1994**, *137*, 2.
(63) Boudaïffa, B.; Cloutier, P.; Hunting, D.; Huels, M. A.; Sanche, L. *Science* **2000**, *287*, 1658.
(64) Martin, F.; Burrow, P. D.; Cai, Z.; Cloutier, P.; Hunting, D.; Sanche, L. *Phys. Rev. Lett.* **2004**, *93*, 068101.
(65) Bao, X.; Wang, J.; Gu, J.; Leszczynski, J. *Proc. Natl. Acad. Sci. U.S.A.* **2006**, *103*, 5658.
(66) Gu, J.; Wang, J.; Leszczynski, J. *J. Am. Chem. Soc.* **2006**, *128*, 9322.
(67) Li, X.; Sevilla, M. D.; Sanche, L. *J. Am. Chem. Soc.* **2003**, *125*, 13668.
(68) Kumar, A.; Sevilla, M. D. *J. Phys. Chem. B* **2007**, *111*, 5464.
(69) Kumar, A.; Sevilla, M. D. *J. Am. Chem. Soc.* **2008**, *130*, 2130.

thus prohibited; at this stage, the proton-transferred structure of $G(N1-H)^{-}:C(N3+H)^{\bullet}$ is not able to capture a second excess electron. Once the hydration reaches the extent that can support the formation of stable $G(N1-H)^{-}:C(N3+H)^{-}$ dianion, the damage on the cytosine sites can once again occur through the mechanisms proposed by the previous computational studies.[3,4] On the basis of this scenario, one can expect the observation of an initial decrease followed by an increase on the yield of SSB at cytosine sites as the hydration increases.

One of the striking findings in the present work is the significant effect of base stacking on the proton transfer in $G:C^{\bullet-}$. Our analyses for $(G:C)_3^{\bullet-}$ clearly indicate that the G:C stacking effect mainly originates from the electrostatic force, namely, the interactions between the dipole moments of peripheral base pairs and the negative charge on the sandwiched base pair, rather than from charge-delocalization effect. If the present finding was valid to all sequences and considering the relatively small dipole moment of A:T base pair (~2 D with negative end on A and positive end on T), one can predict that the rate and extent of the proton transfer decrease in the order of $(C:G)(G:C)^{\bullet-}$(C:G) > $(T:A)(G:C)^{\bullet-}$(T:A) > isolated $(G:C)^{\bullet-}$ > $(A:T)(G:C)^{\bullet-}$(A:T) > $(G:C)(G:C)^{\bullet-}$(G:C). The prediction can be extended to the proton transfer in oxidized $G^{\bullet+}:C$ according to the electrostatic argument; notice that the positive charge now initially resides on G and gradually shifts to C in the course of the proton transfer. It should be aware that the above-mentioned arguments are tenable only when the excess charge is largely confined on the middle G:C base pair. Unfortunately, the nature of excess charge distribution within the DNA duplex is still unclear. While many computational studies demonstrate that the excess charge is nearly localized on a single base pair,[39,41,42,53] there is evidence, on the other hand, supporting the polaron-like behavior in which the excess charge is spread over several base pairs.[70,71]

However, we found experimental results that sustain our prediction about the effect of base sequence on the proton-transfer reaction. In a recent nanosecond pulse radiolysis experiment, Kobayashi et al. systematically investigated the kinetics of deprotonation of guanine radical cation incorporated in oligonucleotide duplexes of various sequences.[33] They considered the deprotonation process being composed of two steps; the first step is a rapid prototropic equilibrium between $G^{\bullet+}:C$ and $G(N1-H)^{\bullet}:C(N3+H)^{+}$, and the second step is a relatively slower process of releasing the an extra proton on $C(N3+H)^{+}$ into the surrounding water. According to the pre-equilibrium approximation, the apparent rate constant of deprotonation can be expressed by a product of the prototropic equilibrium constant and the rate constant of proton abstraction by water. The experimentally observed rate constants of deprotonation display a decreasing order $(C:G)(G:C)^{\bullet+}$(C:G) > $(T:A)(G:C)^{\bullet+}$(T:A) > $(A:T)(G:C)^{\bullet+}$(A:T) > $(A:T)(G:C)^{\bullet+}$(G:C) > $(G:C)(G:C)^{\bullet+}$(G:C). We interpret the trend as a reflection of the prototropic equilibrium within oxidized G:C because it seems very likely that the rate of proton abstraction by surrounding water is sequence independent. If so, the experimental result implies that the extent of equilibrium shifting to the proton-transferred structure $G(N1-H)^{\bullet}:C(N3+H)^{+}$ decreases according to the above order, totally consistent with our prediction based on the electrostatic model. To the best of our knowledge, the corresponding experiment on reduced oligonucleotide duplexes has not appeared yet.

In the calculations of $(dG:dC)_3^{\bullet-}\cdot 5H_2O$, we found that the water molecules do not undergo dramatic rearrangements during the course of the proton transfer (Figure 4). The obvious geometric changes are the distances of the hydrogen bonds between water molecules and nucleobases. The variations of these hydrogen-bond distances correlate closely with the charge transfer between nucleobases. For example, the hydrogen-bond distances of O−H···N3(G), O−H···O6(G), and O−H···N7(G) become shorter and shorter as the negative charge gradually shifts from C to G during the proton transfer; in contrast, an increase of O−H···O2(C) distance is observed (Figure 4). Here we would like to point out that the microhydration structure observed in the $(dG:dC)_3^{\bullet-}\cdot 5H_2O$ is very different from that reported in the water clusters of isolated base and base-pair radical anions. Microhydration structures of isolated bases and base pairs as well as their radical anions have been widely explored by quantum mechanical approaches.[72−78] These studies demonstrate that electron attachment would induce dramatic water rearrangements. In neutrals, water molecules always locate on the lateral side of nucleobases and form hydrogen bonds with each other and/or with nucleobases. Upon electron addition, a common reorganization of water molecules is shifting from the lateral side to the top side of the nucleobases and stabilizing the excess electron by direct interaction with the π-electron cloud; for instance, the H_2O can act as a proton donor to form a hydrogen bond with the N4 atom of the amino group of cytosine from the top side.[72,76] This type of water arrangement is unlikely to occur in the DNA duplex because the top and bottom of an embedded base pair are protected by neighboring base pairs. As demonstrated in the calculations of $(dG:dC)_3^{\bullet-}\cdot 5H_2O$, the water molecules still remain approximately on the lateral side of the G:C radical anion (Figure 4). The difference in the hydration structure should reflect in the hydration effects on the properties of base-pair radical anions.

To assess the effect of different hydration structures on the proton-transfer energetics, additional B3LYP/6-31+G* calculations were carried out for the radical anion of isolated 9-methylguanine-1-methylcytosine (mG:mC) and its pentahydrates. The optimized structures for $(mG:mC)^{\bullet-}\cdot 5H_2O$ exhibit the above-described hydration pattern, in which some of the water molecules interact with the base-pair radical anion from its top side (Figure S2 in Supporting Information). Interestingly, this type of hydration pattern only displays moderate influences on the energetics of the proton transfer; the activation energy and reaction energy decrease by ca. 0.8 and 3 kcal/mol, respectively (Table S1 in Supporting Information). This outcome is in contrast with the calculations of $(dG:dC)_3^{\bullet-}$ and $(dG:dC)_3^{\bullet-}\cdot 5H_2O$, which reveal a significant decrease of ca. 4 and 7 kcal/mol, respectively, for the activation energy and reaction energy (Table 1). These results tell us that the hydration of an isolated base pair can not adequately represent the solvent effects on the properties of a base pair enclosed in DNA duplex. To more realistically mimic the hydration environment experienced by a base pair embedded in DNA, the effect of external structure,

(70) Conwell, E. M. *Proc. Natl. Acad. Sci. U.S.A.* **2005**, *102*, 8795.
(71) Henderson, P. T.; Jones, D.; Hampikian, G.; Kan, Y.; Schuster, G. B. *Proc. Natl. Acad. Sci. U.S.A.* **1999**, *96*, 8353.
(72) Kumar, A.; Sevilla, M. D.; Suhai, S. *J. Phys. Chem. B* **2008**, *112*, 5189.
(73) Kumar, A.; Mishra, P. C.; Suhai, S. *J. Phys. Chem. A* **2005**, *109*, 3971.
(74) Bao, X.; Sun, H.; Wong, N. B.; Gu, J. *J. Phys. Chem. B* **2006**, *110*, 5865.
(75) Bao, X.; Liang, G.; Wong, N. B.; Gu, J. *J. Phys. Chem. A* **2007**, *111*, 666.
(76) Kim, S.; Schaefer, H. F. *J. Chem. Phys.* **2007**, *126*, 064301.
(77) Kim, S.; Schaefer, H. F. *J. Phys. Chem. A* **2007**, *111*, 10381.
(78) Kim, S.; Wheeler, S. E.; Schaefer, H. F. *J. Chem. Phys.* **2006**, *124*, 204310.

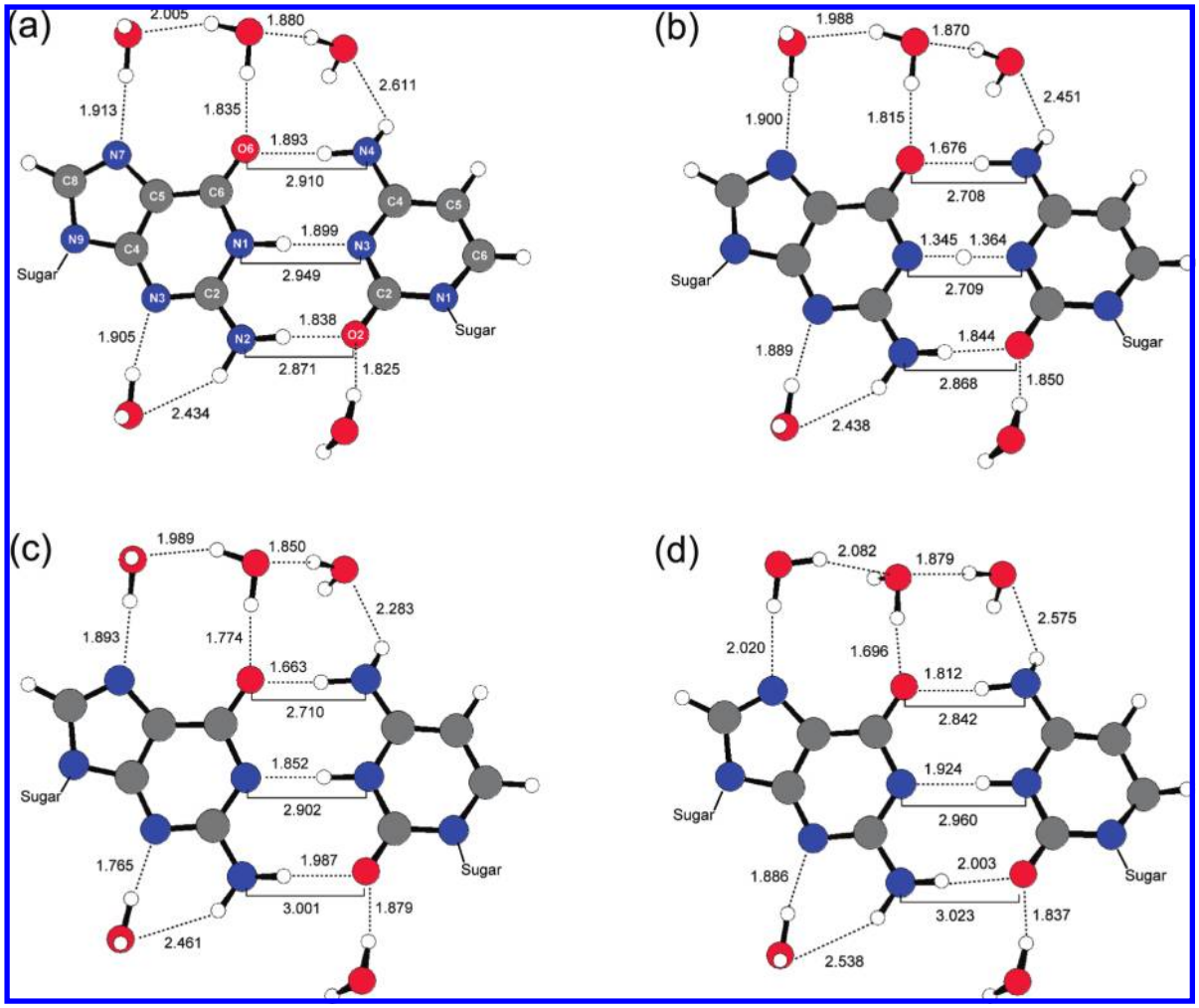

Figure 4. Optimized geometries of $(dG:dC)_3^{\bullet-}\cdot 5H_2O$ at (a) canonical Watson−Crick structure, (b) transition-state structure, (c) proton-transferred structure, and the optimized geometry of (d) $(dG:dC)_3^{-2}\cdot 5H_2O$ dianion. For clarity, the sugar−phosphate backbone and outer base pairs are not shown.

such as the presence of neighboring base pairs and backbone, on the hydration structure has to be taken into consideration.

5. Conclusions

In this study, the proton-transfer reaction within $G:C^{\bullet-}$ embedded in B-form DNA trimer, d(5′-GGG-3′)·d(3′-CCC-5′), has been investigated by quantum mechanical approaches. The environmental effects, including sugar−phosphate backbone, counterions, base stacking, as well as hydration, on the proton transfer in $G:C^{\bullet-}$ were well-separated and analyzed. The following conclusions emerge from our calculations:

(1) Among the four external interactions, the sugar−phosphate backbone and counterions display minor effects, whereas the neighboring base pairs and hydration display important effects on the proton transfer in $G:C^{\bullet-}$.

(2) The proton transfer in base-pair trimer $(G:C)_3^{\bullet-}$ is obviously less easier to proceed than in isolated $G:C^{\bullet-}$. The significant influence of G:C stacking is attributed to the electrostatic interactions between the dipole moments of peripheral G:C pairs and the excess negative charge localized on the middle G:C pair, rather than from charge delocalization among base pairs. The electrostatic model suggests that the rate and extent of the proton transfer in ionized G:C decrease in the order $(C:G)(G:C)^{\bullet\pm}(C:G)$ > $(T:A)(G:C)^{\bullet\pm}(T:A)$ > isolated $(G:C)^{\bullet\pm}$ > $(A:T)(G:C)^{\bullet\pm}(A:T)$ > $(G:C)(G:C)^{\bullet\pm}(G:C)$. The prediction of the sequence effect is tentative and requires further verifications since it is not sure whether the picture of charge localization is valid in all DNA sequences. Nevertheless, there is experimental evidence that supports our prediction.

(3) Hydration greatly facilitates the proton transfer in $G:C^{\bullet-}$. The water molecules in the first hydration shell account for the major part of the hydration effect on the proton-transfer reaction; the further inclusion of bulk hydration only slightly decreases the activation energy and reaction energy of the proton transfer. We notice that the microhydration structure around an embedded $G:C^{\bullet-}$ is different from that around an isolated $G:C^{\bullet-}$ due to the presence of other DNA components. The difference in the microhydration structures can lead to a quite dissimilar solvent effect on the property of a base-pair anion. Therefore, to more closely mimic the hydration environment experienced by a base pair embedded in DNA duplex, one has to consider the effect of external structure, such as the presence of neighboring base pairs and backbone, on the hydration structure.

(4) In contrast to the hydration effect on the proton-transfer reaction, where the water molecules in the first hydration layer play the major role, the inclusion of long-range polarization of water is critical for the formation of stable base-pair dianions. The calculations indicate that a G:C base pair in DNA duplex can accommodate two excess electrons only in aqueous environment.

(5) The medium-range electron-correlation interaction (i.e., dispersion force), although playing a critical role in determination of binding energy for $\pi-\pi$ stacking systems, has negligible influence on the energetics of proton transfer in $(G:C)_3^{\bullet-}$.

(6) Our results in combination with previous studies suggest that the behaviors of excess electron transport and LEE-induced damage in G:C stacks are very sensitive to the degree of hydration. In the circumstance without water, the excess electron on the π^* of cytosine can trigger DNA strand breaks that mainly occur on the C3′−O bond. As the hydration slightly increases to the level that contains the first hydration shell, the proton transfer within $G:C^{\bullet-}$ starts to overcome and suppress the electron transfer along the stack and the strand break as a result of the formation of charge-spin-separated species $G(N1-H)^-:C(N3+H)^{\bullet}$. In the bulk hydration, the $G(N1-H)^-:C(N3+H)^{\bullet}$ becomes able to capture a second excess electron to form a stable $G(N1-H)^-:C(N3+H)^-$ dianion, which can once again lead to DNA damages.

Acknowledgment. We thank the National Science Council of Taiwan for financial support and the National Center for High-Performance Computing for computer time and facilities.

Supporting Information Available: Complete ref 51, figure of ONIOM PESs, figure of microhydrated structures for $(mG:mC)^{\bullet-}\cdot 5H_2O$, energetics of proton transfer in $(mG:mC)^{\bullet-}$ and $(mG:mC)^{\bullet-}\cdot 5H_2O$, Cartesian coordinates of optimized structures. This material is available free of charge via the Internet at http://pubs.acs.org.

JA906899P